Cuff-less Blood Pressure Monitoring in a Cohort of People with Parkinson's Disease

Colum Crowe, Marco Sica, Lorna Kenny, Brendan O'Flynn, David Scott Mueller, Suzanne Timmons, John Barton, Salvatore Tedesco*

***Abstract*—Parkinson's disease is often considered as a "movement disorder". Nevertheless, People with Parkinson's (PwPD) may also experience other non-motor symptoms, such as abnormalities and alterations in blood pressure (BP). Real-time cuffless BP monitoring may help identify the end-users' overall health state and support clinical decision-making, however most of the studies in the field did not investigate PwPD as a possible cohort of reference. To the best of the authors' knowledge, there are no scientific publications, or commercially available wearable solutions, monitoring BP measurements by means of electrocardiogram (ECG) and/or photoplethysmogram (PPG) in a Parkinsonian cohort. Based on a Random Forest (RF) model and a combination of publicly available data and data collected in lab-settings using a wearable prototype developed at Tyndall National Institute, good performance were achieved on both systolic and diastolic BP measurements with a mean absolute error equal to 7.84 ± 8.12 and 7.51 ± 6.16 mmHg, respectively, for PwPD. As BP disorders are highly prevalent in PwPD, and can mimic dopaminergic deficiency, this work is a step forward in the effective management of motor and non-motor symptoms in this complex cohort of patients.**

Keywords—cuff-less blood pressure, blood pressure monitoring, PwPD, Parkinson's, wearable

I. Introduction

Parkinson's disease (PD) is a chronic condition characterized by the degeneration of neurons responsible for the production of dopamine [1]. Although non-motor symptoms also occur, the pronounced impact of PD on motor processes and the increasing loss of autonomy in activities of daily living (ADLs) have led to its classification as a "movement disorder". A wide range of motor symptoms such as tremor, bradykinesia, and dyskinesia can develop concurrently with PD. Numerous research studies have already investigated the accuracy of identifying those motor symptoms using wrist- and/or ankle-worn inertial sensors in combination with machine learning (ML) models [2-5].

Nevertheless, People with Parkinson's (PwPD) may also experience troublesome non-motor symptoms. For instance, both Parkinson's itself and the medications used to treat it can be contributing factors to abnormalities and alterations in blood pressure (BP) [6]. Cardiovascular dysfunction in the form of abnormal BP patterns can occur across all PD stages and contribute to impaired quality of life, disability, and a shorter life expectancy [7], thus necessitating appropriate assessment and management. As a result, precise and regular BP measurements may help identify the end-users' overall health state and support clinical decision-making.

Ambulatory blood pressure monitoring (ABPM) is a better indicator of blood pressure fluctuations than spot measurements recorded in the clinic [8-9]. Indeed, with PD symptoms fluctuating throughout the day, spot BP measurements might not reflect the real BP profile of the patient [7]. ABPM is often performed over periods between 24 and 48 hours, with BP readings being taken using oscillometry every 30 min during the day and every hour at night by increasing and gradually releasing the pressure of an inflatable cuff applied to the arm. This method, however, is cumbersome and can disrupt sleep patterns. Recent advances in non-invasive estimation of BP have been focused on cuff-less approaches using the pulse arrival time (PAT) calculated between the electrocardiogram (ECG) signal and photoplethysmogram (PPG) waveform measured by pulse oximetry at the fingertip [10]. While there is a plethora of works in literature in the last decade, as well as devices on the market, which have successfully investigated the possibility to perform real-time cuffless continuous blood pressure estimation [11-13], most of those studies considered healthy young or middle-aged subjects and did not investigate the possibility to consider PwPD.

To the best of the authors' knowledge, there are no scientific publications, or commercially available wearable solutions specific for PwPD, monitoring BP measurements by means of ECG and/or PPG in a Parkinsonian cohort. Only one study validated the accuracy of the off-the-shelf Samsung SM-R850 (a smartwatch equipped with a PPG sensor and proprietary online algorithms for BP calculation) against a sphygmomanometer in a Parkinsonian cohort [14]. Results reported by Ahn et al. [14] showed accurate results, e.g., 0.4 ± 4.6 and 1.1 ± 4.5 mmHg errors for diastolic BP (DBP) and systolic BP (SBP), respectively, but did not provide details on the proprietary methods used for estimating BP. The objective of this study is therefore to evaluate various supervised ML approaches to estimate blood pressure based on ECG and PPG signals collected from a cuff-less wearable device developed at the Tyndall National Institute in a Parkinsonian cohort. This manuscript focuses specifically on

This work was supported in part by the Enterprise Ireland and AbbVie Ireland NL B.V., under Agreement IP 2017 0625, and in part by the Science Foundation Ireland which are Co-Funded through the European Regional Development Fund under Grant 12/RC/2289-P2-INSIGHT, Grant 13/RC/2077-CONNECT, and Grant 16/RC/3918-CONFIRM.

C. Crowe, M. Sica, B. O'Flynn, J. Barton and S. Tedesco are with the Tyndall National Institute, University College Cork, Lee Maltings Complex, Dyke Parade, T12R5CP Cork, Ireland.

L. Kenny, and S. Timmons are with the Centre for Gerontology and Rehabilitation, University College Cork, Cork, Ireland.

D.S. Mueller is with AbbVie Inc., Chicago, Illinois, United States.

* Corresponding author. e-mail: salvatore.tedesco@tyndall.ie

2023 IEEE Sensors Applications Symposium (SAS) | 979-8-3503-2307-8/23/$31.00 ©2023 IEEE | DOI: 10.1109/SAS58821.2023.10253995

the machine learning modelling aspects required for estimating blood pressure based on ECG and PPG signals, while the evaluation of the hardware prototype monitoring device is out of the scope of the paper. The manuscript is structured as follows: Section II presents the datasets employed in the study and brief indications on the hardware adopted. Section III illustrates the developed methods. In Section IV, the results of each approach are presented in detail, along with a discussion on the strengths and weakness of each approach.

II. Datasets Employed

A. Public Dataset

The Cuff-Less Blood Pressure Estimation Data Set created by Kachuee et al. [15] and available on UCI Machine Learning Repository was used as a starting point for the analysis. This dataset consists of 12,000 instances of ECG and PPG signals, and invasive arterial blood pressure (ABP) – e.g., a form of invasive blood pressure monitoring carried out through the cannulation of a peripheral artery - signals collected at 125 Hz from 851 patients monitored at various hospitals between 2011 and 2008, which were selected from Physionet's Multiparameter Intelligent Monitoring in Intensive Care online waveform database (MIMIC II) and pre-processed according to the methodology described in [16]. A visual representation of the data distribution of the dataset is shown in Figure 1 (top).

B. Tyndall WESAA Dataset

A second dataset (WESAA - Wearable Enabled Symptom Assessment Algorithms) was collected and consisted of ECG and PPG signals recorded with a wearable prototype device developed at the Tyndall National Institute, as well as discrete DBP, SBP, and mean arterial pressure (MAP) -e.g., the average arterial pressure throughout one cardiac cycle, systole and diastole - readings measured at 167Hz by a clinically validated off-the-shelf cuff (Withings BPM Connect, WiFi Smart Blood Pressure Monitor [17]). The manufacturer's guidelines for positioning and placement of the cuff [18] were followed for each measurement and carried out by trained operators to ensure a consistent data collection process. The developed hardware prototype consists of two identical devices worn on the most affected wrist and ankle; each device contains a rechargeable battery, inertial sensors, and PPG and ECG sensors. At the patient's request (double-pressing a button), PPG and ECG data can be gathered from the wrist location for roughly 30 seconds (at 125 Hz). Figure 2 shows an example of the device in operation.

The participants included 18 healthy (14 males / 4 females) subjects and 10 PwPD (details in Table I), each of whom first took three BP measurements with the gold-standard cuff and the average recorded for comparison. The trial then consisted of six 30 second measurements with the prototype with the subject sitting (two measurements at the index finger, two at the thumb, and two at the less affected side). A visual representation of the distribution of the dataset is in Figure 1 (bottom). The study received approval by the Clinical Research Ethics Committee (CREC) of the Cork Teaching Hospitals at the University College Cork (Reference: ECM 4 (r) 11/02/2020 & ECM 3 (hh) 17/05/2022).

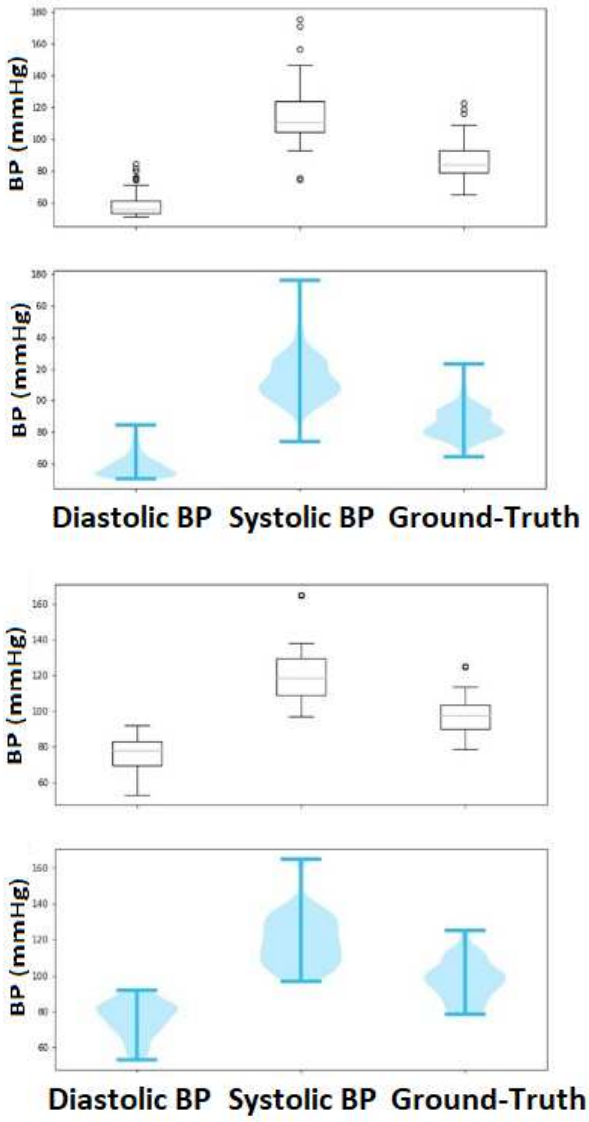

Figure 1. (Top) Boxplot and violinplot showing distribution of diastolic blood pressure DBP (left), systolic blood pressure SBP (middle), and ground-truth arterial blood pressure ABP data (right) from dataset in [15-16]; (Bottom) Boxplot and violinplot showing distribution of diastolic blood pressure DBP (left), systolic blood pressure SBP (middle), and ground-truth mean arterial pressure MAP data (right) from the Tyndall WESAA dataset

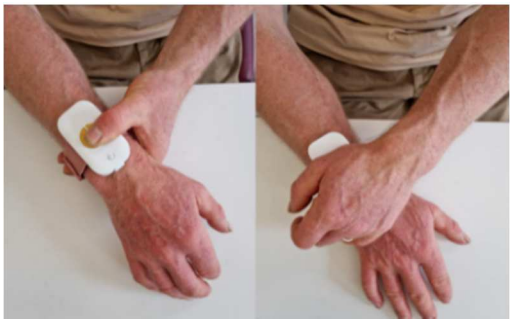

Figure 2. Wearable prototype used for data collection

TABLE I. PWPD CHARACTERISTICS

#	Gender	Age	Height (cm)	Weight (Kg)	Affected Side	Hoehn and Yahr (Stage)	Years since diagnosis	Unified Parkinson's Disease Rating Scale
1	F	73	171	70	L	II	9	78
2	M	72	183	90	R	III	10	69
3	M	64	173	82	L	III	7	102
4	M	78	172	69	L	III	7	87
5	F	70	165	70	L	I	4	60
6	M	72	168	82	L	II	2	55
7	M	72	173	75	L	II	6	62
8	F	62	170	95	L	I	9	38
9	F	59	175	70	L	I	6	38
10	F	73	170	63	L	III	15	64

III. METHODOLOGY

The continuous ABP signal was used for the calculation of the discrete SBP and DBP target values in the case of the Kachuee dataset while the measurements from the BP cuff were used for the data collected by the WESAA prototype. The signal envelope of the ABP was computed using the Two-stage Zero-order Holding (TZH) processing technique proposed in [19]. The median of the upper and lower bounds of the signal envelope were then used for the systolic and diastolic values respectively. The ECG and PPG signals were segmented into windows of 5 seconds with 50% overlap and temporal and morphological features were extracted from the processed data (Table II and Figure 3) [20]. The Kachuee dataset was split 80% (training) and 20% (test set) and a grid-search was performed using 5-fold cross-validation on the training set. Different regression models were tested (linear regression, Support Vector Machine -SVM, Random Forest - RF, and XGBoost) and optimized for the k best features (k = 1-39) selected according to the F-value between label and feature. The chosen model was validated on the 20% test set and on 100% of WESAA to estimate SBP and DBP. Secondly, the WESAA dataset was split 80% vs. 20% into a training and test set and a grid-search was performed using the same method. The chosen model was validated on the 20% test set. Finally, the two available datasets were merged to form a combined dataset and the grid-search process was repeated. The chosen model was validated on the WESAA data present in the 20% test set and the entire test set. Mean Absolute Error (MAE) was used as a scoring metric for all the evaluations.

IV. RESULTS AND DISCUSSION

The results for the carried out investigations are shown in Tables III-V. Table III shows the validation scores of different models following a 5-fold cross-validation on the training set of the two datasets adopted and a third case in which the two datasets are combined. Score results are presented as an average between SBP and DBP to ensure that the model performs a trade-off optimizing for both parameters at the same time. It is evident that RF was the best performing model in training consistently across the datasets using 5-fold cross-validation (5.65 mmHg for the dataset in [15], and 6.95 mmHg for the WESAA dataset). Linear and SVM regression models selected less features than the tree-based models, thus indicating that they may be less prone to overfitting. Based on this analysis RF models were used for the following investigations.

Table IV shows the results specifically for the diastolic BP evaluation. The model was trained on the training set obtained from the Kachuee dataset and tested on the test set in the same dataset, showing good results with a MAE equal to 3.53 ± 4.09 mmHg. However, as expected, results did not generalize well to the WESAA dataset overall (either on the control subjects or the PwPD) showing MAE scores of 14.15 ± 8.67 and 13.64 ± 7.63 mmHg, respectively. Therefore, comparable results are shown between PwPD and controls subjects. This could be potentially explained by the different sensors used for data collection of the ECG and PPG signals, or more likely by the different approach used to obtain the BP measurement labels across the two datasets. On the other hand, the models that were trained using data only from the WESAA dataset typically performed better, with slightly better performance on control subjects (4.97 ± 5.09 mmHg) than on PwPD (7.31 ± 5.89 mmHg). Combining the two datasets (with training data including data from both [15] and WESAA) allowed a reduction in MAE scores and more homogeneous results across the different cohorts (e.g., MAE: 7.51 ± 6.16 mmHg on WESAA PwPD subjects, MAE: 6.36 ± 6.50 mmHg on WESAA control subjects, and MAE: 5.66 ± 6.01 mmHg on the testing set of the combined datasets). Thus, MAE went from a 4.97 – 7.31 mmHg range (e.g., 2.34 mmHg of difference) with WESAA only dataset to a 5.66 – 7.51 mmHg range (e.g., 1.85 mmHg of difference) when combining the two sets.

Similar results are obtained for the systolic BP (Table V). The model trained on [15] did not generalize well to the WESAA dataset (MAE: 14.44 ± 12.45 mmHg for WESAA PD subjects, MAE: 14.57 ± 11.78 mmHg for WESAA controls, vs. MAE: 6.50 ± 7.93 mmHg for test set from Kachuee dataset). The models trained using data only from the WESAA dataset showed better performance (MAE: 8.10 ± 9.98 mmHg for PD subejcts, and 7.48 ± 7.16 mmHg for controls). Combining the two datasets allowed for more homogeneous results across the different cohorts (MAE: 7.84 ± 8.12 mmHg on WESAA PwPD subjects, MAE: 8.29 ± 7.62 mmHg on WESAA control subjects, and MAE: 7.98 ± 8.53 mmHg on the test set of the combined data). Thus, MAE went from a 7.48 – 8.10 mmHg range (e.g., 0.62 mmHg of difference) with WESAA only dataset to a 7.84 –8.29 mmHg range (e.g., 0.45 mmHg of difference) when combining the two datasets.

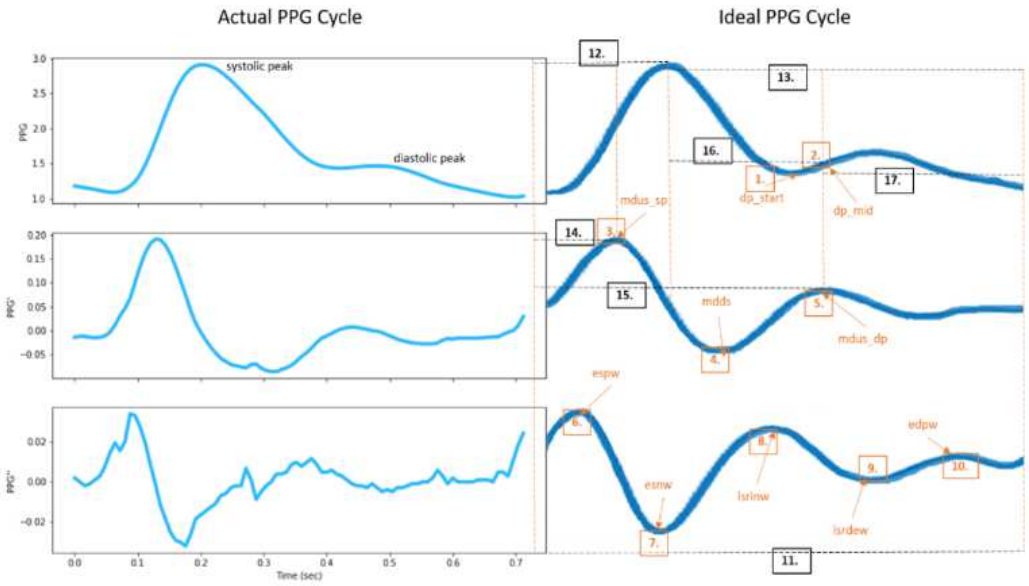

Figure 3. Temporal and morphological features (from #1 to #17) extracted from each of the PPG signals

TABLE II. DESCRIPTION OF THE TEMPORAL AND MORPHOLOGICAL FEATURES EXTRACTED FROM THE PPG AND ECG SIGNALS

#	*Feature Description*	#	*Feature Description*
1	index of the diastolic slope (its middle point) (dp_mid)	21	$\frac{PPG^{*}[esnw]\text{-}PPG^{*}[lsrinw]\text{-}PPG^{*}[lsrdew]}{PPG^{*}[espw]}$
2	index of the starting point of the diastolic slope (dp_start)	22	$\frac{PPG^{*}[esnw]\text{-}PPG^{*}[lsrinw]\text{-}PPG^{*}[lsrdew]\text{-}PPG^{*}[edpw]}{PPG^{*}[espw]}$
3	maximum derivative of the upslope between the start of the signal and the systolic peak (mdus_sp)	23	$\frac{PPG'[lsrinw]}{PPG'[mdus_{sp}]}$
4	relevant minimum after mdus_sp, representing the knee of the original ppg signal (mdds)	24	$\frac{sum(PPG'[sys_{peak}:lsrdew]^2)}{sum(PPG'^2)}$
5	peak after the valley at mdds, representing the maximum upslope of the diastolic rise/ledge (mdus_dp)	25	$\frac{PPG[lsrinw]}{PPG[sys_{peak}]}$
6	early systolic positive wave (espw)	26	(AUC from start of cycle to max upslope point) + (AUC from max upslope point to systolic peak)
7	early systolic negative wave (esnw)	27	Area above the curve (AAC) from start of cycle to systolic peak
8	late systolic re-increasing wave (lsrinw)	28	AUC from systolic peak to diastolic rise) + AUC from diastolic rise to end of cycle
9	late systolic re-decreasing wave (lsrdew)	29	AAC from systolic peak to end of cycle
10	early diastolic positive wave representing the dicrotic notch of the original ppg signal (edpw)	30	maximum of FFT
11	cycle duration time	31	frequency corresponding to dom_freq_magnitude
12	time from cycle start to systolic peak	32	$\frac{\text{sum of FFT around dom}_{freq}}{\text{sum of FFT}}$
13	time from systolic peak to cycle end	33	spectral flatness
14	time from cycle start to first peak in PPG'	34	entropy of FFT
15	time from cycle start to second peak in PPG' (dicrotic notch)	35	entropy
16	time from systolic peak to dicrotic notch	36	skewness
17	time from dicrotic notch to cycle end	37	kurtosis
18	$\frac{PPG'[lsrdew]\text{-}PPG'[esnw]}{lsrdew - esnw}$	38	pulse arrival time
19	$\frac{sum(PPG'[sys_{peak}:lsrinw]^2)}{sum(PPG'^2)}$	39	time between r peaks
20	$\left(\frac{1}{sampling\_rate}\right)*(lsrinw\text{-}sys_{peak})$		

TABLE III. MAE SCORES (IN MMHG) ON TRAINING SET FOR THE TWO DATASETS – AVERAGE OF SBP AND DBP

Model	***Kachuee Dataset [15]***	***WESAA Dataset***	***Combined Datasets***
Linear Regression	8.68 (k=3)	9.46 (k=33)	10.07 (k=15)
SVM	8.92 (k=3)	9.91 (k=1)	10.26 (k=4)
Random Forest	**5.65 (k=39)**	**6.95 (k=36)**	**6.99 (k=38)**
XGBoost	6.51 (k=39)	7.79 (k=39)	8.32 (k=38)

TABLE IV. DIASTOLIC BP SCORES (MAE AND SD - IN MMHG)

	Trained on Kachuee Dataset [15]	***Trained on WESAA Dataset***	***Trained on Combined Datasets***
Tested on Kachuee Dataset [15]	3.53 ± 4.09	-	-
Tested on WESAA Dataset (PD)	13.64 ± 7.63	7.31 ± 5.89	7.51 ± 6.16
Tested on WESAA Dataset (Controls)	14.15 ± 8.67	4.97 ± 5.09	6.36 ± 6.50

	Trained on Kachuee Dataset [15]	*Trained on WESAA Dataset*	*Trained on Combined Datasets*
Tested on Combined Dataset (Controls)	-	-	5.66 ± 6.01

TABLE V. SYSTOLIC BP SCORES (MAE AND SD - IN MMHG)

	Trained on Kachuee Dataset [15]	*Trained on WESAA Dataset*	*Trained on Combined Datasets*
Tested on Kachuee Dataset [15]	6.50 ± 7.93	-	-
Tested on WESAA Dataset (PD)	14.44 ± 12.45	8.10 ± 9.98	7.84 ± 8.12
Tested on WESAA Dataset (Controls)	14.57 ± 11.78	7.48 ± 7.16	8.29 ± 7.62
Tested on Combined Dataset (Controls)	-	-	7.98 ± 8.53

Overall, the present investigation showed promising results in the implementation of a machine learning model for cuff-less BP monitoring in a Parkinsonian's cohort. As BP disorders are highly prelevant in PwPD, this work is a step forward in effective symptom management in this complex cohort of patients.

It was also shown that, in order to ameliorate the issues generally related to small datasets in lab settings, combining different datasets adopting the same targeted variables (e.g., ECG, PPG signals) strengthen the overall consistent model performance allowing for a more generalizable model (as shown by the limited difference in performance in the various use cases analysed) applicable to different sets of subjects (PwPD and healthy controls), thus also showing the benefits for open access data. While data merging has proved effective in addressing issues related to small datasets in several studies [21-22] for microarray datasets, tabular data, and time series data, to the best of the authors' knowledge, this is the first time that the benefits of data merging to model fitting have been shown also for blood pressure monitoring.

From a clinical perspective, despite the promising results, the performance shown indicates that such a model could be used mostly for evaluation of intraday BP fluctuations rather than as a clinical tool. Moreover, the present model has been built using data collected only with subjects in static conditions (i.e., sitting) and not during dynamic movements. This data is, however, still very useful in PD, where differentiation of symptoms due to dopaminergic deficiency versus hypotension can be challenging (e.g., in post prandial fatigue), where the absolute BP value is less important than the trend in BP values.

Future work should explore alternative window configurations for signal segmentation, incorporating additional temporal and morphological features, evaluating different dataset splitting strategies or considering other datasets, and employing bayesian optimization techniques for hyper-parameter selection. These additional studies are required to further improve the model performance and robustness so that the developed model could be used in real-world scenarios for clinical-grade minute-to-minute BP assessments, thus supporting the clinical decision-making process by trained operators.

REFERENCES

[1] T. Foltynie, C. Brayne, R. A. Barker, "The heterogeneity of idiopathic Parkinson's disease," J. Neurol., 249, 2, 138–145, 2002

[2] J.G.V. Habets et al., "Rapid dynamic naturalistic monitoring of bradykinesia in parkinson's disease using a wrist-worn accelerometer," Sensors, 21, 23, 2021

[3] N. Mahadevan et al., "Development of digital biomarkers for resting tremor and bradykinesia using a wrist-worn wearable device," npj Digit. Med., 3, 1, 2020

[4] R. San-Segundo et al., "Parkinson's disease tremor detection in the wild using wearable accelerometers," Sensors, 20, 20, 1–23, 2020

[5] M.D. Hssayeni, et al., "Dyskinesia estimation during activities of daily living using wearable motion sensors and deep recurrent networks," Sci. Rep., 11, 1, 2021

[6] T. Tsukamoto, et al., "Blood pressure fluctuation and hypertension in patients with Parkinson's disease," Brain Behav., 3, 6, 710-714, 2013

[7] D. Tulbă, et al., "Blood pressure patterns in patients with Parkinson's disease: A systematic review," J Pers Med., 11, 2, 129, 2021

[8] E. Finnegan et al., "Pulse arrival time as a surrogate of blood pressure," Sci Rep, 11, 1, 1–21, 2021

[9] Z. Haider Janjua, et al., "Knowledge-driven feature engineering to detect multiple symptoms using ambulatory blood pressure monitoring data," Comput Meth Prog Bio, 2022

[10] S.N.A. Ismail, et al., "Recent advances in non-invasive blood pressure monitoring and prediction using a machine learning approach," Sensors, 22, 16, 6195, 2022

[11] X. Ding, et al., "Pulse transit time based continuous cuffless blood pressure estimation: A new extension and a comprehensive evaluation," Sci Rep, 7, 11554, 2017

[12] Y.H. Li, et al., "Real-time cuffless continuous blood pressure estimation using deep learning model," *Sensors, 20*, 5606, 2020

[13] T. Athaya, S. Choi, "Real-time cuffless continuous blood pressure estimation using 1D squeeze U-Net model: A progress toward mHealth," Biosensors, 12, 8, 655, 2022

[14] J.H. Ahn, et al., "Validation of blood pressure measurement using a smartwatch in patients with Parkinson's disease," Front Neurol., 2021

[15] M. Kachuee, et al., "Cuff-less high-accuracy calibration-free blood pressure estimation using pulse transit time," IEEE Int Symp Circ Syst ISCAS*,* 1006-1009, 2015

[16] M. Kachuee, et al., "Cuffless blood pressure estimation algorithms for continuous health-care monitoring," IEEE Trans Biomed Eng, 2017

[17] https://www.withings.com/us/en/bpm-connect (Online: 21/01/2023)

[18] https://support.withings.com/hc/en-us/articles/360024481313-BPM-Connect-Positioning-myself-and-the-BPM-for-the-measurement (Online: 26/05/2023)

[19] F.P.W. Lo, et al., "Continuous systolic and diastolic blood pressure estimation utilizing long short-term memory network," Int. Conf. IEEE Eng. Med. Biol. Soc. EMBS, 1853–1856, 2017

[20] G. Slapnicar, et al., "Blood pressure estimation from photoplethysmogram using a spectro-temporal deep neural network," Sensors, 19, 15, 2019

[21] V. Lagani, et al., "A comparative evaluation of data-merging and meta-analysis methods for reconstructing gene-gene interactions," BMC Bioinformatics, 17 (Suppl 5), S194, 2016

[22] T. Nguyen, et al. "Combining datasets to increase the number of samples and improve model fitting, " arXiv:2210.05165 [stat.ML]